

Journal of Materials Chemistry A

Accepted Manuscript



This is an *Accepted Manuscript*, which has been through the Royal Society of Chemistry peer review process and has been accepted for publication.

Accepted Manuscripts are published online shortly after acceptance, before technical editing, formatting and proof reading. Using this free service, authors can make their results available to the community, in citable form, before we publish the edited article. We will replace this *Accepted Manuscript* with the edited and formatted *Advance Article* as soon as it is available.

You can find more information about *Accepted Manuscripts* in the [Information for Authors](#).

Please note that technical editing may introduce minor changes to the text and/or graphics, which may alter content. The journal's standard [Terms & Conditions](#) and the [Ethical guidelines](#) still apply. In no event shall the Royal Society of Chemistry be held responsible for any errors or omissions in this *Accepted Manuscript* or any consequences arising from the use of any information it contains.



Journal Name

Benzothiadiazole Based Conjugated Polymers for High Performance Polymer Solar Cells

Received 00th January 20xx,
Accepted 00th January 20xx

Xue Gong, Guangwu Li, Cuihong Li,* Jicheng Zhang and Zhishan Bo*

DOI: 10.1039/x0xx00000x

www.rsc.org/

Three novel copolymers **P1-3** with alkylthiophenylsubstituted benzodithiophene as the donor unit, thiophene as the spacer, and benzothiadiazole as the acceptor unit have been designed, synthesized, and used as donor materials for polymer solar cells. Polymer solar cells with the **P3**:PC₇₁BM blends as the active layer exhibited a high power conversion efficiency (PCE) of 7.7% and a good tolerance to the change of film thickness. PCE higher than 7.3% can be obtained with the thickness of active layer ranging from 90 to 380 nm, indicating that **P3** is a very promising donor material for practical application.

Introduction

Polymer solar cells (PSCs) have been attracted an intensive research interest due to their unique characteristics such as light weight, flexible, and roll to roll processability.¹ By material design, interfacial modification and device optimization, power conversion efficiency (PCE) of polymer solar cells (PSCs) has been dramatically improved to more than 11% in the last two decades.²⁻⁴ However, due to the relatively low hole mobility of polymer materials, most high efficiency polymer donor materials are very sensitive to the thickness of active layer. For most high efficiency polymer materials, the optimal thickness of active layer is around 100 nm. Increasing the thickness of active layer usually leads to a dramatic decrease of the PCE. For practical applications, it is quite difficult to fabricate defect free PSCs with an active layer thickness of about 100 nm by roll to roll process. Only a limited number of conjugated polymers, which can produce high efficiency in a thick active layer, were reported.⁵⁻¹⁴ Therefore, it is quite important to develop new polymer donor materials that can still have high efficiency with a thicker active layer. Donor-acceptor (D-A) design for conjugated polymers has been proved to be an efficient strategy to finely tune the energy levels of conjugated polymers.¹⁵⁻²² Benzo[1,2-b:4,5-b']dithiophene (BDT) is a commonly used donor unit for the synthesis of low band gap polymers and small molecules used for high performance polymer/organic solar cells.²³⁻²⁸ PCE higher than 10% has been achieved in single junction devices based on BDT containing polymers and small molecules.^{29,30} For BDT based polymers, introducing two-dimensional (2-D) conjugated side chain has been proved to be an efficient strategy to achieve high device performance. The influence of side chains on the performance of PSCs has been intensively investigated.³¹⁻³⁵ Recently, alkylthiothienyl group has been

demonstrated to be a better substituent for BDT based polymers due to the weaker electron donating ability of sulfur atom.³⁵⁻³⁷ Additionally, conjugated polymers bearing the lateral alkylphenyl substituents could also afford high performance solar cells.^{21,38} Here we designed and synthesized three new conjugated polymers, in which benzodithiophene bearing two alkylthiophenyl side chains as the donor unit, benzothiadiazole derivatives as the acceptor unit, and thiophene as the spacer. PSCs based on **P1** and **P2**, which contain 5,6-bis(alkyloxy)benzothiadiazole acceptor unit, gave PCEs of 5.4% and 6.1%, respectively. PSCs based on **P3**, which contains 5-alkyloxy-6-fluorobenzothiadiazole acceptor unit, exhibited the highest PCE of 7.7%. Most importantly, a PCE of 7.3% can still be achieved for **P3** based PSCs with an active layer thickness of 378 nm, demonstrating that **P3** is a very promising polymer for practical applications.

Results and discussion

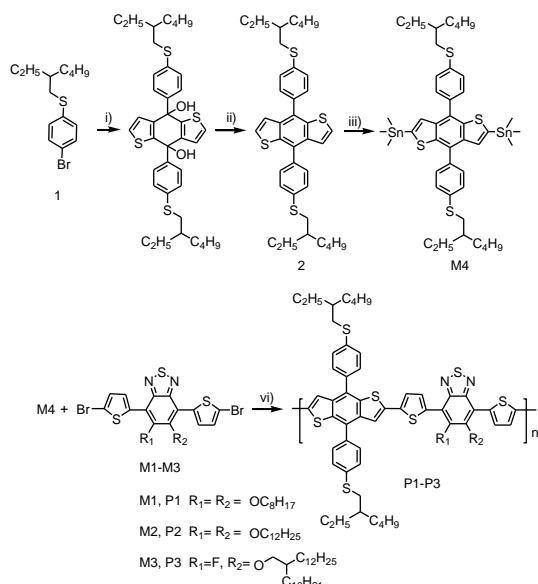
Material Synthesis and Characterization

The syntheses of monomer **M4** and copolymers **P1-3** are shown in Scheme 1. The treatment of compound **1** with *n*-BuLi at -78 °C was followed by quenching the formed aryl lithium with benzo[1,2-b:4,5-b']dithiophene-4,8-dione to afford the diol, which was converted to compound **2** in a total yield of 39% by the treatment with SnCl₂ and dilute hydrochloric acid. The subtraction of two hydrogen atoms on compound **2** with *n*-BuLi at -78 °C was followed by reaction with trimethyltin chloride to afford **M4** in a yield of 90%. **M1**, **M2** and **M3** were prepared according to literature.³⁹⁻⁴¹ Three copolymers **P1-3** were synthesized in yields of 62-96% by Stille poly condensation of **M1**, **M2** and **M3** with **M4**, respectively, using Pd(PPh₃)₄ as catalyst precursor in a solvent mixture of toluene and DMF at 110 °C under the protection of nitrogen atmosphere. During the polymerization, part of the polymers precipitated from the reaction mixture and the precipitated polymer chains cannot further grow, leading to a broad molecular weight distribution. Since **P1**, carrying two octyloxy substituents on the benzothiadiazole unit, exhibits the poorest solubility among these three polymers, therefore it has the

Beijing Key Laboratory of Energy Conversion and Storage Materials, College of Chemistry, Beijing Normal University, Beijing 100875, China. Email: zsbo@bnu.edu.cn; licuihong@bnu.edu.cn.
Electronic Supplementary Information (ESI) available. See DOI: 10.1039/x0xx00000x

largest polydispersity index (PDI) among these three polymers (vide infra). Although these copolymers exhibited limited solubility in chlorobenzene (CB), 1,2-dichlorobenzene (DCB), and 1,2,4-trichlorobenzene (TCB) at room temperature, they could become fully soluble at elevated temperature.

Scheme 1. Synthetic routes of monomer M4 and copolymers P1-3



i) *n*-BuLi, benzo[1,2-*b*:4,5-*b'*]dithiophene-4,8-dione, -78 °C; ii) SnCl₄·H₂O, HCl, rt; iii) *n*-BuLi, SnMe₃Cl, -78 °C; iv) Pd(PPh₃)₄, toluene/DMF (5:1 by volume), reflux.

The number average molecular weight (M_n) and PDI of copolymers were determined by GPC at 80 °C using TCB as an eluent and narrow distributed polystyrenes as the calibration standards, and the results are summarized in Table 1. It's worth noting that high molecular weight polymers were obtained, which are beneficial to achieve high photovoltaic performance.

Table 1. Molecular Weights and Thermal Properties of the Copolymers

polymer	M_n (kg/mol) ^a	M_w (kg/mol) ^a	PDI	T_d (°C) ^b
P1	41.5	211.5	5.09	300
P2	77.9	225.3	2.88	300
P3	54.5	196.7	3.60	310

^a M_n , M_w , and PDI of polymers were determined by GPC at 150 °C using polystyrene standards with 1,2,4-trichlorobenzene as an eluent. ^b Decomposition temperatures were determined by TGA under N₂ based on 5% weight loss

Thermogravimetric analysis (TGA) showed that all polymers are of good thermal stability with the 5% decomposition temperature up to 300 °C for **P1**, 300 °C for **P2**, and 310 °C for **P3** under a nitrogen atmosphere (Fig. S1, supporting information). Differential scanning calorimetry (DSC) measurement showed that only **P3** had clear melting and recrystallization peaks located at approximately 165 °C and 120 °C, respectively (Fig. S2, supporting information). No obvious glass transition was detected for **P1** and **P2** by differential scanning calorimetry (DSC) measurements in the range of 50 to 250 °C. As shown in Fig. 1, **P1-3** exhibit almost

the same powdery X-ray diffraction (XRD) curves in the wide angle region with the broad diffraction peaks located at 2θ of 24.29 °, 23.78° and 24.07°, respectively. The π - π stacking distances between polymer backbones are therefore calculated to be 3.66 Å for **P1**, 3.74 Å for **P2** and 3.70 Å for **P3**.

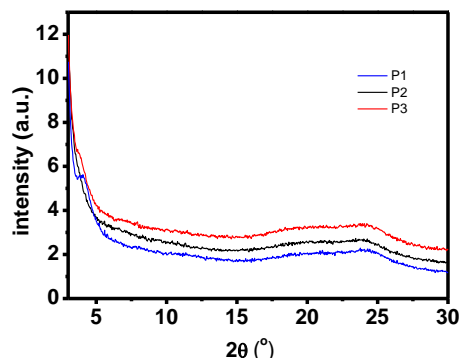
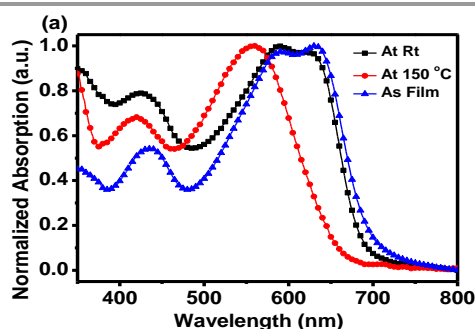


Fig. 1 XRD curves of polymers powdery samples

Optical and electrochemical properties

The optical properties of **P1-3** were investigated by UV-vis absorption spectroscopy and their absorption spectra are shown in Fig. 2. All three polymers exhibit a broad absorption in the range of 350-700 nm. As shown in Fig. 2a, the absorption spectra of **P1** in dilute DCB solution at room temperature and as thin films showed similar profiles with three peaks located at 425, 588 and 628 nm. After the solution was heated to about 150 °C, the absorption spectrum of **P1** blue shifted and became much narrower. Such a phenomenon indicates that **P1** forms aggregation even in dilute solution at room temperature, and the aggregates can be dissociated to form real solution at elevated temperature. In comparison with the solution absorption spectrum of **P1** at 150 °C, the film one exhibited a red-shift of about 73 nm with the absorption onset at 692 nm. The optical band gap ($E_{g,opt}$) of **P1** was therefore calculated to be 1.79 eV, according to the equation: $E_{g,opt} = 1240/\text{absorption onset}$. As for **P2**, its optical properties are quite similar to that of **P1** as demonstrated in Fig. 2b. Similarly, $E_{g,opt}$ of **P2** is calculated to be 1.78 eV. The absorption spectra of **P3** in DCB solution at 150 °C, in DCB solution at room temperature, and as thin films are shown in Fig. 2c. In going from solution at 150 °C to thin films, the absorption spectra of **P3** are gradually red-shifted. The above results demonstrated that **P3** forms real solution at 150 °C in DCB solution, after cooled down to room temperature the polymer chains form weaker aggregates, and as thin films the aggregation is further enhanced. The different behaviour for **P3** is probably due to its better solubility in DCB solution than that of **P1** and **P2**.



This journal is © The Royal Society of Chemistry 20xx

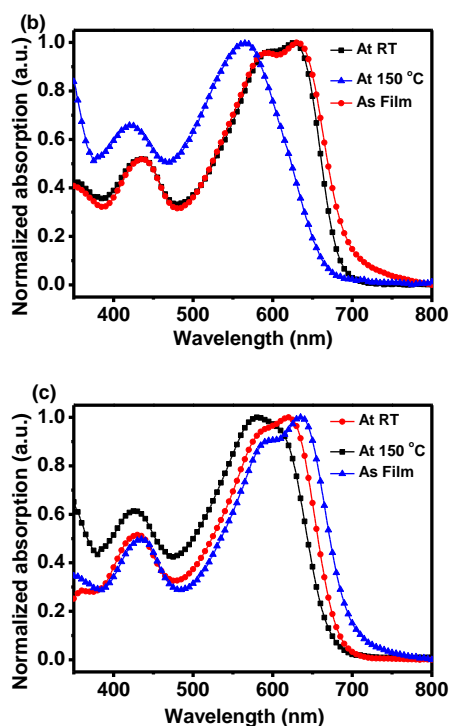


Fig. 2 UV-vis absorption spectra of **P1** (a), **P2** (b), and **P3** (c) in DCB solutions at room temperature, at 150 °C, and as films.

The electrochemical properties of **P1-3** were investigated by cyclic voltammetry (CV) using a standard three electrodes electrochemical cell.

As shown in Fig. 3, these three polymers exhibited quasi reversible redox processes. The onset oxidation potentials of polymer films for **P1**, **P2** and **P3** are 0.71, 0.70, and 0.89 V, respectively. HOMO levels of **P1**, **P2**, and **P3** were determined, using the equation $E_{\text{HOMO}} = -e(E_{\text{ox}} + 4.71)$, to be -5.42, -5.41, and -5.60 eV, respectively. LUMO levels of **P1**, **P2** and **P3** were therefore calculated according to the equation $E_{\text{LUMO}} = E_{\text{HOMO}} + E_{\text{g,opt}}$ to be -3.63, -3.63 and -3.84 eV, respectively. In comparison with **P1** and **P2** with 5,6-bis(alkyloxy)benzothiadiazole as the acceptor unit, **P3** with 5-fluoro-6-alkyloxybenzothiadiazole as the acceptor unit exhibits not only slightly broader absorption spectrum but also lower HOMO and LUMO levels.

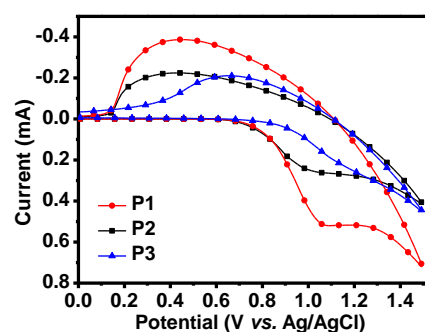


Fig. 3 Cyclic voltammograms of **P1**, **P2** and **P3** as films on a platinum electrode in 0.1 mol/L Bu₄NPF₆acetonitrile solution at a scan rate of 100 mV/s.

Table 2. Optical and electrochemical properties of **P1**, **P2** and **P3**.

polymer	$\lambda_{\text{max}}(\text{nm})^{\text{a}}$	$\lambda_{\text{max}}(\text{nm})^{\text{b}}$	$\lambda_{\text{edge}}(\text{nm})^{\text{b}}$	$E_{\text{g,opt}}(\text{eV})^{\text{c}}$	HOMO (eV)	LUMO(eV) ^d
P1	423, 557	436, 636	692	1.79	-5.42	-3.63
P2	422, 565	437, 631	695	1.78	-5.41	-3.63
P3	427, 580	435, 636	703	1.76	-5.60	-3.84

^a Insolutions at 150 °C; ^b As film; ^c Calculated from the absorption band edge of copolymer films, $E_{\text{g,opt}} = 1240/\lambda_{\text{edge}}$. ^d Calculated by the equation $E_{\text{LUMO}} = E_{\text{HOMO}} + E_{\text{g,opt}}$.

Photovoltaic Properties.

To evaluate the photovoltaic performance of **P1-3**, PSCs with a device structure of indium tin oxide (ITO)/poly(3,4-ethylenedioxythiophene):poly(styrene sulfonate) (PEDOT:PSS)/active layer/LiF/Al were fabricated. Firstly, devices with an active layer thickness of about 100 nm were fabricated to optimize the weight ratio of polymer to PC₇₁BM. For **P1** and **P2**, devices fabricated from DCB solutions in a polymer:PC₇₁BM weight ratio of 1:2.5 gave the best performance. A PCE of 5.4% with a V_{oc} of 0.74 V, a J_{sc} of 11.60 mA/cm² and an FF of 0.63 for **P1** and a PCE of 6.1% with a V_{oc} of 0.76 V, a J_{sc} of 11.26 mA/cm² and an FF of 0.72 for **P2** were obtained. For **P3**, devices fabricated in a polymer to PC₇₁BM weight ratio of 1:2

from DCB solution gave the best performance with a PCE of 5.7%, a V_{oc} of 0.84 V, a J_{sc} of 9.38 mA/cm², and an FF of 0.72. The results are summarized in Table S1. Solvent additives such as 1,8-diiodooctane (DIO) and 1-chloronaphalene (1-CN) were used in different concentrations to further optimize the film morphology of active layer. Only for **P3**, the use of DIO (2.0%, by volume) as the processing additive has a positive effect. PCE of polymer solar cells can be markedly enhanced to 7.4% with a V_{oc} of 0.82 V, a J_{sc} of 12.28 mA/cm², and an FF of 0.73. J-V curves of devices under simulated solar illumination (AM1.5G, 100 mW/cm²) are shown in Fig. 4 with the corresponding parameters summarised in Table 3.



Journal Name

Table 3. Device performances of P1 and P2 under optimized conditions and P3 without or with solvent additive

Polymer	Thickness (nm)	Solvent	PCE	V_{oc} [V]	J_{sc} [mA/cm ²]	FF	SCLC mobilities
P1	93	DCB	5.4%	0.74	11.60	0.63	9.5-E5
P2	110	DCB	6.1%	0.76	11.26	0.72	1.2-E5
P3	95	DCB	5.7%	0.84	9.38	0.72	5.0-E5
P3	89	DCB ^a	7.4%	0.82	12.28	0.73	6.0-E2

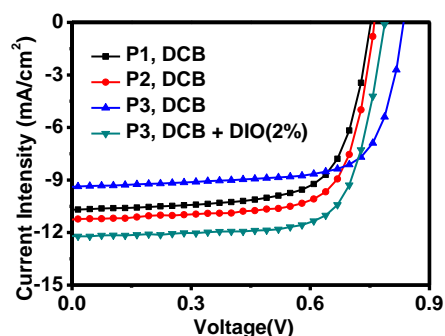
^a 2% DIO by volume

Fig. 4 J-V curves of P1, P2 and P3 under optimized condition.

After the preliminary optimization, the thickness of active layer was further screened. It was difficult to obtain thick active layer for P1 due to its limited solubility in hot DCB. For P2, after the thickness of active layer increased to about 220 nm, the J_{sc} enhanced to 13.18 mA/cm², the FF decreased to 0.59, and the PCE decreased to 5.7%. For P3, after the thickness of active layer increased to 250 nm, devices gave the best performance with a PCE of 7.7%, a J_{sc} of 14.33 mA/cm², a V_{oc} of 0.79 V, and an FF of 0.69. Further increasing the thickness of active layer to 378 nm, the J_{sc} increased to 15.12 mA/cm², but the FF decreased to 0.60, leading to a slightly decreased PCE of 7.3%. Even increasing the thickness of active layer to 480 nm, devices still gave a PCE of 6.6% with the J_{sc} slightly decreased to 14.84 mA/cm² and an FF of 0.57. It is worth noting that efficiencies higher than 7.3% can be achieved for devices with a thickness in the range of 90 to 380 nm. The detailed device characters including standard deviations are summarized in Table 4, indicating that P3 is a very promising donor material for practical applications. To further understand the unique behaviour of P3, hole mobilities of blend films were measured by space charge limited current (SCLC) method and the data are summarized in Table 4. The hole mobility of P3 based blend films was calculated to be 3 orders higher than P1 and

P2 based blend films. Such a high hole mobility for the P3:PC₇₁BM blend films is consistent with the high PCE of P3 based PSCs even with an active layer thickness up to about 500 nm. High hole mobility is beneficial for the efficient charge separation and transportation.

Table 4. The photovoltaic characteristics of P2 and P3 with thick active layers.

Polymer	PCE (average)	Standard deviation	V_{oc} [V]	J_{sc} [mA/cm ²]	FF	Thickness (nm)
P2	5.7% (5.4%)	0.22	0.73	13.18	0.59	217
P3	7.4% (7.1%)	0.19	0.82	12.28	0.73	89
P3	7.6% (7.3%)	0.17	0.80	13.71	0.70	180
P3	7.7% (7.6%)	0.10	0.79	14.33	0.69	250
P3	7.3% (7.0%)	0.23	0.80	15.12	0.60	378
P3	6.6% (6.4%)	0.19	0.79	14.84	0.57	480

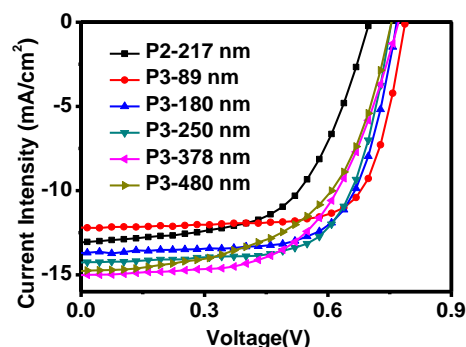


Fig. 5 J-V curves of P2 and P3 with thick active layers.

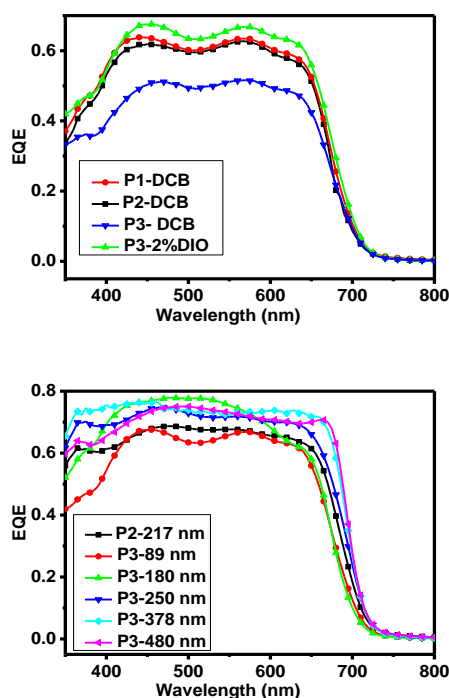


Fig. 6 External quantum efficiencies (EQEs) of the P1-3 devices

As shown in Fig. 6, the external quantum efficiencies (EQEs) of the P1-3 devices fabricated under the optimized conditions were measured and used to verify the accuracy of the J_{sc} values from the J-V measurements. The J_{sc} values obtained by integrating the EQE curves with the AM 1.5G solar spectrum agreed well with the J_{sc} values from J-V measurement, namely the difference is within 5%.

The morphology of active layer plays a very crucial rule to the performance of PSCs, high efficiency PSCs require that the polymer donor and PC₇₁BM acceptor form bicontinuous networks, which have large interfacial area and phase-separated domain size of 10-20 nm, can facilitate exciton dissociation and charge transport. Therefore the film morphology of active layers was investigated by transmission electron microscopy (TEM) and the images are shown in Fig. 7. As shown in Fig. 7a and 7b, the P1:PC₇₁BM and P2:PC₇₁BM blend films fabricated from DCB solutions formed relatively homogenous films with sparse large domains, and no obvious nanoscale phase separation can be observed. As shown in Fig. 7c, the P3:PC₇₁BM blend films fabricated from pure DCB solutions exhibited a large scale phase separation. The dark domains are probably PC₇₁BM aggregations and the lighter ones are probably polymer aggregates. After the addition of DIO (2.0%, by volume) as the processing additive, the P3:PC₇₁BM blend films became much more homogenous, nanofibrils and bicontinuous interpenetrating networks were formed as shown in Fig. 7d. The morphology of P3:PC₇₁BM blend films obviously benefits the charge dissociation and transportation, leading to a high hole mobility and a high efficiency even the thickness of active layer is up to 480 nm.

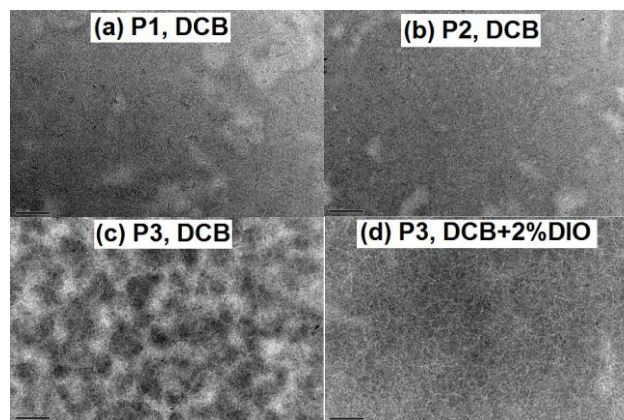


Fig. 7 TEM images of (a) P1:PC₇₁BM in weight ratio of 1: 2.5; (b) P2:PC₇₁BM in weight ratio of 1: 2.5; (c) P3:PC₇₁BM in weight ratio of 1:2; (d) P3:PC₇₁BM in weight ratio of 1:2 with 2% DIO as additive. The scale bar was 200 nm.

Conclusions

Three novel copolymers P1-3 with benzodithiophene bearing two alkylthiophenyl side chains as the donor unit, thiophene as the spacer, and benzothiadiazole as the acceptor unit have been designed, synthesized and characterized. BHJ PSCs fabricated with P1-3 as the donor and PC₇₁BM as the acceptor in a thickness of about 100 nm afforded high device performances with PCEs up to 5.4% for P1, 6.1% for P2 and 7.4% for P3. Only for the mono fluoro substituted benzothiadiazole based P3, the PCE of devices is insensitive to the thickness of active layer. Devices with an active layer thickness of 250 nm gave the best PCE of 7.7%. Even the thickness of active layer increased to 480 nm, devices still gave a PCE of 6.4%. The good tolerance to the thickness of active layer made P3 a very promising donor material for practical applications.

Acknowledgements

We express thanks for the financial support by the NSF of China (51003006 and 21161160443), the 973 Programs (2011CB935702), and the Fundamental Research Funds for the Central Universities.

Notes and references

The authors declare no competing financial interest.

1. L. T. Dou, J. B. You, Z. R. Hong, Z. Xu, G. Li, R. A. Street and Y. Yang, *Adv. Mater.*, 2013, **25**, 6642-6671.
2. C. C. Chen, W. H. Chang, K. Yoshimura, K. Ohya, J. B. You, J. Gao, Z. R. Hong and Y. Yang, *Adv. Mater.*, 2014, **26**, 5670-5677.
3. Z. C. He, C. M. Zhong, S. J. Su, M. Xu, H. B. Wu and Y. Cao, *Nat. Photonics*, 2012, **6**, 591-595.
4. S. J. Liu, K. Zhang, J. M. Lu, J. Zhang, H. L. Yip, F. Huang and Y. Cao, *J. Am. Chem. Soc.*, 2013, **135**, 15326-15329.
5. Z. Chen, P. Cai, J. Chen, X. Liu, L. Zhang, L. Lan, J. Peng, Y. Ma and Y. Cao, *Adv. Mater.*, 2014, **26**, 2586-2591.
6. H. Choi, S.-J. Ko, T. Kim, P.-O. Morin, B. Walker, B. H. Lee, M. Leclerc, J. Y. Kim and A. J. Heeger, *Adv. Mater.*, 2015, **27**, 3318-3324.

7. J. W. Jung, T. P. Russell and W. H. Jo, *ACS Appl. Mater. Interfaces*, 2015, **7**, 13666-13674.
8. R. Kroon, A. Diaz de Zerio Mendaza, S. Himmelberger, J. Bergqvist, O. Bäcke, G. C. Faria, F. Gao, A. Obaid, W. Zhuang, D. Gedefaw, E. Olsson, O. Inganäs, A. Salleo, C. Müller and M. R. Andersson, *J. Am. Chem. Soc.*, 2014, **136**, 11578-11581.
9. W. Li, S. Albrecht, L. Yang, S. Roland, J. R. Tumbleston, T. McAfee, L. Yan, M. A. Kelly, H. Ade, D. Neher and W. You, *J. Am. Chem. Soc.*, 2014, **136**, 15566-15576.
10. S. C. Price, A. C. Stuart, L. Q. Yang, H. X. Zhou and W. You, *Journal of the American Chemical Society*, 2011, **133**, 4625-4631.
11. X. Zhu, J. Fang, K. Lu, J. Zhang, L. Zhu, Y. Zhao, Z. Shuai and Z. Wei, *Chem. Mater.*, 2014, **26**, 6947-6954.
12. Y. Liu, J. Zhao, Z. Li, C. Mu, W. Ma, H. Hu, K. Jiang, H. Lin, H. Ade and H. Yan, *Nat. Commun.*, 2014, **5**, 5293.
13. T. L. Nguyen, H. Choi, S. J. Ko, M. A. Uddin, B. Walker, S. Yum, J. E. Jeong, M. H. Yun, T. J. Shin, S. Hwang, J. Y. Kim and H. Y. Woo, *Energy Environ. Sci.*, 2014, **7**, 3040-3051.
14. N. Wang, Z. Chen, W. Wei and Z. Jiang, *J. Am. Chem. Soc.*, 2013, **135**, 17060-17068.
15. E. Zhou, S. Yamakawa, K. Tajima, C. Yang and K. Hashimoto, *Chem. Mater.*, 2009, **21**, 4055-4061.
16. D. Veldman, S. C. J. Meskers and R. A. J. Janssen, *Adv. Funct. Mater.*, 2009, **19**, 1939-1948.
17. F. Huang, K.-S. Chen, H.-L. Yip, S. K. Hau, O. Acton, Y. Zhang, J. Luo and A. K. Y. Jen, *J. Am. Chem. Soc.*, 2009, **131**, 13886-13887.
18. J. Roncali, *Acc. Chem. Res.*, 2009, **42**, 1719-1730.
19. D. Yang, Z. Guang, L. Yang, Y. Huang, Q. Wei, Z. Lu and J. Yu, *Sol. Energ. Mater. Sol. C.*, 2012, **105**, 220-228.
20. L. Huo, S. Zhang, X. Guo, F. Xu, Y. Li and J. Hou, *Angew. Chem. Int. Ed.*, 2011, **50**, 9697-9702.
21. M. J. Zhang, X. Guo, W. Ma, S. Q. Zhang, L. J. Huo, H. Ade and J. H. Hou, *Adv. Mater.*, 2014, **26**, 2089-2095.
22. M. L. Keshtov, D. V. Marochkin, V. S. Kochurov, A. R. Khokhlov, E. N. Koukaras and G. D. Sharma, *J. Mater. Chem. A*, 2014, **2**, 155-171.
23. Y. Liang, D. Feng, Y. Wu, S.-T. Tsai, G. Li, C. Ray and L. Yu, *J. Am. Chem. Soc.*, 2009, **131**, 7792-7799.
24. L. T. Dou, J. Gao, E. Richard, J. B. You, C. C. Chen, K. C. Cha, Y. J. He, G. Li and Y. Yang, *J. Am. Chem. Soc.*, 2012, **134**, 10071-10079.
25. J. Zhou, Y. Zuo, X. Wan, G. Long, Q. Zhang, W. Ni, Y. Liu, Z. Li, G. He, C. Li, B. Kan, M. Li and Y. Chen, *J. Am. Chem. Soc.*, 2013, **135**, 8484-8487.
26. Y. Chen, X. Wan and G. Long, *Acc. Chem. Res.*, 2013, **46**, 2645-2655.
27. Y. Zhang, S. K. Hau, H.-L. Yip, Y. Sun, O. Acton and A. K. Y. Jen, *Chem. Mater.*, 2010, **22**, 2696-2698.
28. Y. Liu, C.-C. Chen, Z. Hong, J. Gao, Y. Yang, H. Zhou, L. Dou, G. Li and Y. Yang, *Sci. Rep.*, 2013, **3**, 3356.
29. S. H. Liao, H. J. Jhuo, P. N. Yeh, Y. S. Cheng, Y. L. Li, Y. H. Lee, S. Sharma and S. A. Chen, *Sci. Rep.*, 2014, **4**, 6813.
30. Z. C. He, B. Xiao, F. Liu, H. B. Wu, Y. L. Yang, S. Xiao, C. Wang, T. P. Russell and Y. Cao, *Nat. Photonics*, 2015, **9**, 174-179.
31. G. Li, B. Zhao, C. Kang, Z. Lu, C. Li, H. Dong, W. Hu, H. Wu and Z. Bo, *ACS Appl. Mater. Interfaces*, 2015, **7**, 10710-10717.
32. C. Y. Yu, B. T. Ko, C. Ting and C. P. Chen, *Sol. Energ. Mater. Sol. C.*, 2009, **93**, 613-620.
33. J. Yuan, L. Xiao, B. Liu, Y. F. Li, Y. H. He, C. Y. Pan and Y. P. Zou, *J. Mater. Chem. A*, 2013, **1**, 10639-10645.
34. L. Ye, S. Q. Zhang, L. J. Huo, M. J. Zhang and J. H. Hou, *Acc. Chem. Res.*, 2014, **47**, 1595-1603.
35. L. Ye, S. Q. Zhang, W. C. Zhao, H. F. Yao and J. H. Hou, *Chem. Mater.*, 2014, **26**, 3603-3605.
36. C. H. Cui, W. Y. Wong and Y. F. Li, *Energy & Environ. Sci.*, 2014, **7**, 2276-2284.
37. Z. Zheng, S. Q. Zhang, M. J. Zhang, K. Zhao, L. Ye, Y. Chen, B. Yang and J. H. Hou, *Adv. Mater.*, 2015, **27**, 1189-1194.
38. M. J. Zhang, Y. Gu, X. Guo, F. Liu, S. Q. Zhang, L. J. Huo, T. P. Russell and J. H. Hou, *Adv. Mater.*, 2013, **25**, 4944-4949.
39. R. Qin, W. Li, C. Li, C. Du, C. Veit, H.-F. Schleiermacher, M. Andersson, Z. Bo, Z. Liu, O. Inganäs, U. Wuerfel and F. Zhang, *J. Am. Chem. Soc.*, 2009, **131**, 14612-14613.
40. G. Li, C. Kang, X. Gong, J. Zhang, C. Li, Y. Chen, H. Dong, W. Hu, F. Li and Z. Bo, *Macromolecules*, 2014, **47**, 4645-4652.
41. Z. B. Lim, B. Xue, S. Bomma, H. Li, S. Sun, Y. M. Lam, W. J. Belcher, P. C. Dastoor and A. C. Grimsdale, *J. Polym. Sci. Part A: Polym. Chem.*, 2011, **49**, 4387-4397.

Graphic Abstract

Benzothiadiazole Based Conjugated Polymers for High Performance Polymer Solar Cells

Xue Gong, Guangwu Li, Cuihong Li,* Jicheng Zhang and Zhishan Bo*

Beijing Key Laboratory of Energy Conversion and Storage Materials, College of Chemistry, Beijing Normal University, Beijing 100875, China. Email: zsbo@bnu.edu.cn; licuihong@bnu.edu.cn.

New benzothiadiazole based conjugated polymers have been synthesized as donor materials for high efficiency polymer solar cells with a thick active layer.

